https://doi.org/10.5194/essd-2026-511
Preprint. Discussion started: 21 September 2026

Open Access Earth System Science Data Discussions

The Global Database of Deep-time Sedimentary Mercury Concentrations and Isotope Compositions (DeepSedHg)

Yuchen Yang[1], Songjing Li[1], Wang Zheng[1], Yi Liu[1], Jiubin Chen[1], Ruoyu Sun[1*]

[1] Institute of Surface-Earth System Science, School of Earth System Science, Tianjin University; Tianjin 300072, China.

Correspondence to: Ruoyu Sun (ruoyu.sun@tju.edu.cn)

Abstract. Mercury (Hg) concentrations and isotope compositions preserved in sedimentary successions provide important information for investigating long-term Hg cycling, volcanism, environmental perturbations, and Earth-system evolution. During the past decade, the rapid expansion of sedimentary Hg research has generated a large volume of concentration and isotope data. However, these data remain dispersed across individual studies and are reported using heterogeneous stratigraphic frameworks, metadata conventions, and analytical formats, limiting their accessibility and large-scale reuse. Here we present DeepSedHg (Deep-time Sedimentary Mercury Concentrations and Isotope Compositions) database, a comprehensive global compilation of published sedimentary Hg concentrations and isotope records spanning approximately 2.7 billion years of Earth history. DeepSedHg version 1.0 integrates data from 199 peer-reviewed publications published between 2010 and February 2026 and contains 28264 sample-level records. The database includes 27,990 Hg measurements, of which 3,736 contain both concentration and isotope data. Each record is accompanied by standardized metadata describing stratigraphy, numerical age, lithology, depositional environment, geographic location, paleogeographic position, and associated geochemical parameters. All records were subjected to systematic data harmonization and quality-control procedures, including duplicate screening, metadata verification, chronostratigraphic standardization, coordinate validation, and consistency checks of geochemical variables. The resulting database provides broad temporal, spatial, and environmental coverage of sedimentary Hg records and is distributed in a machine-readable format together with comprehensive metadata documentation. DeepSedHg is publicly available through Zenodo (https://doi.org/10.5281/zenodo.20713398) and an online tool (https://deepsedhg.pages.dev), which is intended to support future synthesis studies, meta-analyses, data-driven investigations, and interdisciplinary research on Hg cycling and environmental change throughout Earth history.

1 Introduction

Mercury (Hg) is a volatile, toxic and redox-sensitive trace element that links geochemical processes across the lithosphere, atmosphere, hydrosphere, and biosphere (Driscoll et al., 2013; Obrist et al., 2018; Pyle and Mather, 2003; Selin, 2009; Sonke et al., 2023). Because Hg can be efficiently emitted to the atmosphere, transported over long distances, and subsequently deposited into terrestrial and marine environments, sedimentary archives preserve valuable records of Hg cycling through

https://doi.org/10.5194/essd-2026-511
Preprint. Discussion started: 21 September 2026

Earth history (Grasby et al., 2019). In particular, anomalous Hg enrichments in sedimentary successions have been extensively employed as proxies for enhanced volcanic emissions associated with large igneous provinces (LIPs) and other major magmatic events (Gong et al., 2024; Zhou et al., 2024). Such Hg anomalies have been reported from numerous geological intervals and are commonly examined in conjunction with mass extinction, climatic perturbations, and changes in marine redox conditions (Grasby et al., 2019; Percival et al., 2021; Shen et al., 2021, 2023; Sun et al., 2023).

Beyond concentration measurements, Hg stable isotopes provide additional information on Hg sources, transport pathways, and transformation processes (Blum et al., 2014; Blum and Bergquist, 2007; Kwon et al., 2020; Sun et al., 2023; Yin et al., 2014). Mercury isotopes include both mass-dependent fractionation (MDF), commonly expressed as δ^{202}Hg, and mass-independent fractionation (MIF), expressed using odd-mass isotopes (Δ^{199}Hg and Δ^{201}Hg) for odd-MIF and even-mass isotopes (Δ^{200}Hg and Δ^{204}Hg) for even-MIF. These isotope signatures have been increasingly applied to distinguish among volcanic, atmospheric, terrestrial, and marine Hg sources and to evaluate photochemical and redox processes within ancient Earth-surface environments (Gong et al., 2024; Sun et al., 2023; Yager et al., 2021; Zheng et al., 2018, 2023; Zhou et al., 2024).

During the past two decades, advance in analytical techniques of Hg isotopes and the growing application of Hg geochemistry in Earth-system studies have resulted in a rapid increase in both Hg concentration and isotope datasets. Hundreds of sedimentary sections spanning a wide range of depositional environments and geological ages have now been investigated, generating a substantial body of published observations. However, these data remain dispersed across individual publications and are commonly reported using different stratigraphic frameworks, age models, metadata conventions, and analytical reporting formats. Although several review articles and thematic compilations have summarized aspects of sedimentary Hg research (Gong et al., 2024; Grasby et al., 2019; Li et al., 2024; Zhou et al., 2024), no standardized database currently exists that systematically integrates deep-time sedimentary Hg concentration and isotope records within a unified temporal, stratigraphic, and geographic framework.

The lack of standardized data integration limits the broader application of published Hg records. Large-scale syntheses of temporal variation, spatial distributions, and long-term trends in Hg cycling require substantial effort to reconcile inconsistent age assignments, lithological classifications, geographic information, and geochemical metadata among studies. Furthermore, incomplete metadata and inconsistent reporting standards reduce data interoperability and constrain the implementation of FAIR (Findable, Accessible, Interoperable, Reusable) data principles (Wilkinson et al., 2016). These challenges highlight the need for a comprehensive data principles and standardized database that consolidates sedimentary Hg records across geological time.

To address this need, we developed DeepSedHg (Deep-time Sedimentary Mercury Concentrations and Isotope Compositions) database, a global compilation of published sedimentary Hg concentrations and isotope data spanning the late Archean to the present (~0–2700 Ma). The current release (v1.0) integrates data from 199 peer-reviewed publications published between January 2010 and February 2026 and contains 28,264 individual sample-level records. The database incorporates Hg concentrations, Hg isotope compositions, stratigraphic information, age assignments, lithological descriptions, depositional

https://doi.org/10.5194/essd-2026-511
Preprint. Discussion started: 21 September 2026

Open Access Earth System Science Data Discussions

settings, geographic coordinates, and associated geochemical parameters within a unified framework. DeepSedHg v1.0 is available in CSV format on Zenodo (https://doi.org/10.5281/zenodo.20713398, Yang et al., 2026), and dynamic updates will be maintained annually by our research group. An online tool for initial data visualization and extraction is provided at: https://deepsedhg.pages.dev.

DeepSedHg was designed to facilitate the discovery, comparison, visualization, and reuse of sedimentary Hg data across multiple spatial and temporal scales. By combining Hg concentration and isotope data with standardized metadata, the database provides a foundation for investigating long-term Hg cycling, evaluating environmental change through Earth history, and conducting data-driven analyses of sedimentary Hg archives. In the following sections, we describe the procedures used for data compilation, harmonization, and technical validation (section 2), present the structure (section 3) and coverage (section 4) of the database, and discuss its usability, limitations, and potential applications (section 5).

2 Data compilation, harmonization, and validation

2.1 Literature survey and data acquisition

DeepSedHg was developed through a systematic compilation of published sedimentary Hg concentration and isotope data. Literature sources were identified primarily through Web of Science and Google Scholar using combinations of keywords including "mercury", "Hg", "mercury isotope", "Hg concentration", "δ^{202}Hg", "Δ^{199}Hg", "mass-independent fractionation", and names of specific geological intervals and environmental events. Additional publications were identified through reference tracking of review articles and relevant Hg geochemical studies.

The literature survey covered studies published from January 2010 to February 2026. The year 2010 was selected as the starting point because Sial et al. (2010) represents one of the earliest deep-time applications of sedimentary Hg chemostratigraphy, using Hg concentrations in Neoproterozoic cap carbonates to explore volcanism-related environmental perturbations. A publication was included if it reported at least sedimentary Hg concentration data or sedimentary Hg isotope data. Studies focusing solely on modern environmental monitoring, pollution assessment, laboratory experiments, biological materials, ores, igneous or metamorphic rocks, or other non-sedimentary materials were excluded. Modern and Holocene sediment records, especially records from the recent ~10 kyr, were included only when they were dated sedimentary archives relevant to geological or paleoenvironmental reconstruction rather than local contamination assessment. Review papers and synthesis articles were not treated as independent data sources unless they contained previously unpublished measurements.

For each eligible publication, data were extracted from manuscript tables, supplementary files, and online repositories, and figures when raw data were not provided. All data were manually entered and independently checked against the original source materials to minimize transcription errors. Potential duplicate records were flagged during compilation and evaluated during the technical validation procedure described below.

https://doi.org/10.5194/essd-2026-511
Preprint. Discussion started: 21 September 2026

Open Access Earth System Science Data Discussions

As of version 1.0, DeepSedHg contains 28,264 individual sample-level records compiled from 199 peer-reviewed publications, representing the most comprehensive collection of deep-time sedimentary Hg concentration and isotope data currently available.

2.2 Data harmonization and standardization

Data originating from different publications were reported using diverse formats, terminologies, units, age models, and metadata conventions. To ensure interoperability and facilitate cross-study analyses, all records were harmonized within a unified database framework. Each row in DeepSedHg corresponds to a sample-level observation. Original sample names, section names, and stratigraphic identifiers were retained wherever possible to maintain traceability to the source publication. However, field names and metadata descriptors were standardized to ensure consistency across studies. No interpolation, extrapolation, gap filling, or statistical imputation was applied during database construction. Missing values remain blank to preserve the integrity of the original observations.

2.2.1 Geochemical standardization

Mercury concentrations were standardized to parts per billion (ppb). Hg isotope compositions were reported following the convention of Blum and Bergquist (2007), with Hg isotope ratios expressed as δ notations and MIF values expressed as Δ notations relative to the NIST SRM 3133 Hg reference standard. Isotope parameters, including δ^{199}Hg, δ^{200}Hg, δ^{201}Hg, δ^{202}Hg, δ^{204}Hg, Δ^{199}Hg, Δ^{200}Hg, Δ^{201}Hg, Δ^{204}Hg, were reported in per mil (‰).
Reported analytical uncertainties were preserved whenever available. For Hg isotope measurements, published 2σ uncertainties were compiled as independent database fields. In cases uncertainties were not explicitly presented, 2σ uncertainties of the sample measurements were not included, which can be estimated according to the principle of iGOS4M (Hg isotope dataset of modern environments) (Sonke et al., 2026). Because uncertainty for Hg concentration measurements was inconsistently reported among studies, concentration uncertainties, which were mostly within ±10% of reported Hg concentrations, were not standardized within the current database. Hg concentration measurements in the source studies were commonly based on established total-Hg analytical approaches, including EPA method-1631 (U.S. Environmental Protection Agency, 2002) via cold-vapor atomic fluorescence spectroscopy (CVAFS) and EPA method-7473 (U.S. Environmental Protection Agency, 2007) via atomic adsorption spectrophotometry (AAS), whereas Hg isotope compositions were all measured by multi-collector inductively coupled plasma mass spectrometry (MC-ICP-MS).

2.2.2 Derived parameters

Several commonly used Hg-normalization indices were included to facilitate comparison among different lithologies and depositional environment, including Hg/TOC, Hg/TS, and Hg/Al ratios. These ratios are commonly used to evaluate the influence of organic matter, sulfide phases, and detrital or clay-rich components on Hg enrichment, and to distinguish primary Hg enrichments from host-phase effects (Fendley et al., 2024; Frieling, 2023). When these indices were reported in

https://doi.org/10.5194/essd-2026-511
Preprint. Discussion started: 21 September 2026

the original publication, published values were retained. When sufficient information was available but the indices were not explicitly reported, values were calculated directly from the corresponding geochemical measurements.

2.2.3 Chronostratigraphic standardization

A unified chronostratigraphic framework was adopted to facilitate temporal comparisons among datasets. Numerical ages were standardized using the International Chronostratigraphic Chart (ICS GTS v2024/12) (Cohen et al., 2025). Published age models were retained whenever reliable numerical constraints were available. Stratigraphic assignments reported using local or regional terminology were translated into globally recognized chronostratigraphic units whenever possible. Each record was assigned standardized temporal attributes, including era, period, epoch, stage, formation, and numerical age (Ma).

2.2.4 Geographic standardization

Modern geographic coordinates were standardized using the WGS84 coordinate reference system. When latitude and longitude values were explicitly reported, the published coordinates were adopted directly. For studies lacking numerical coordinates, approximate locations were reconstructed from maps, locality descriptions, and supplementary information provided by the authors. Paleogeographic coordinates were reconstructed using the GPlates Web Service and the PALEOMAP plate reconstruction model (Scotese, 2021). Paleolatitude and paleolongitude were calculated from modern coordinates and assigned numerical ages. Because uncertainties in paleogeographic reconstructions increase substantially prior to the breakup of Rodinia, paleocoordinates were generated only for records younger than 720 Ma. Older records retain modern geographic coordinates only.

2.3 Technical validation and quality control

The technical validation workflow adopted for DeepSedHg follows principles similar to those used in recent isotope compilations, including modern Hg isotope database iGOS^{4}M (Sonke et al., 2026) and deep-time sedimentary nitrogen isotope database DSMS-NI (Du et al., 2026), while incorporating additional procedures tailored to the characteristics of deep-time sedimentary Hg records.

In detail, quality control procedures were implemented throughout all stages of database construction, including data extraction, harmonization, metadata integration, and final compilation. First, all extracted values were checked against the original publications to verify numerical accuracy, sample identity, stratigraphic assignments, and metadata consistency. Randomized secondary checks were performed after database integration to identify transcription errors and formatting inconsistencies. Second, duplicate screening was conducted at both publication and sample levels. Potential duplicate entries were identified through combinations of sample identifiers, section names, stratigraphic positions, coordinates, ages, and bibliographic information. When duplicate records were detected, the original source or the most complete dataset was retained. Third, geographic metadata were validated through automated range checks and manual inspection. Latitude values were required to fall between −90° and 90°, and longitude values between −180° and 180°. Records with potentially

https://doi.org/10.5194/essd-2026-511
Preprint. Discussion started: 21 September 2026

inconsistent coordinates were cross-checked against published locality descriptions. Fourth, age information was evaluated for consistency with assigned chronostratigraphic units. Numerical ages were compared against reported eras, periods, epochs, and stages to identify discrepancies resulting from differing age models or transcription errors. Fifth, Hg concentration and isotope data were examined using frequency distributions, scatter plots, and age-series visualizations. Extreme values were not automatically excluded. Instead, all apparent outliers were verified against original publications and retained when supported by analytical documentation or geological context. Finally, metadata completeness was assessed during database construction. Records lacking essential geological context, such as stratigraphic assignment, depositional setting, or source information, were excluded from the final release. The resulting database provides a traceable, internally consistent, and quality-controlled resource suitable for large-scale analyses of Hg concentrations and isotope compositions throughout Earth history.

3 Database structure

DeepSedHg v1.0 contains 28,264 sample-level records compiled from 199 peer-reviewed publications. Each record represents a single observation and is linked to standardized metadata fields. The database is distributed in a machine-readable comma-separated value (CSV) format and is organized using a standardized tabular structure designed to facilitate data discovery, filtering, integration, and reuse. The current release contains 109 database fields describing data provenance, spatial information, temporal constraints, lithological characteristics, depositional environments, and geochemical measurements. To improve usability and interoperability, field names follow standardized conventions to facilitate automated processing and integration with statistical, geospatial, and Earth-system analysis workflows. The database structure was designed to support FAIR data principles by improving data discoverability, interoperability, and long-term reusability. All records remain directly traceable to their original publications through bibliographic metadata and DOI references.

Figure 1 illustrates the overall architecture of DeepSedHg. Database variables are organized into five major fields: reference information, geographic information, chronostratigraphic information, lithological and depositional information, and geochemical information. A complete description of all database fields, units, and definitions is described below.

https://doi.org/10.5194/essd-2026-511
Preprint. Discussion started: 21 September 2026

Open Access Earth System Science Data Discussions

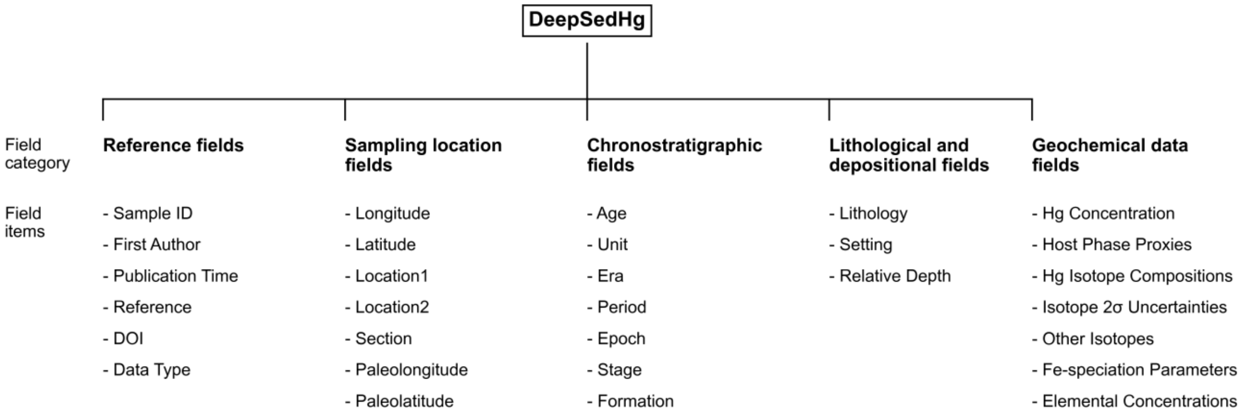

Figure 1: The overall structure of the DeepSedHg database

3.1 Reference information

Reference fields include Sample Identifier, First Author, Publication Time, Reference, Digital Object Identifier (DOI), and Data Type. The original Sample Identifier reported by source studies were retained whenever available, allowing users to directly link database entries to published datasets. Bibliographic fields including First Author, Publication Time, Reference, and DOI provide transparent attribution and facilitate verification of individual records. The Data Type field distinguish among Hg concentration records, Hg isotope records, and records containing both measurement types. These fields establish the provenance framework of DeepSedHg and support reproducibility and data reuse.

3.2 Geographic information

Geographic fields describe both the modern and reconstructed geographic locations of sampling sites. The fields include Longitude, Latitude, Location1, Location2, Section, Paleolongitude and Paleolatitude. Latitude and Longitude represent modern geographic coordinates based on the WGS84 reference system. When coordinates were unavailable in the original publication, they were estimated from published maps and locality descriptions. Location1 and Location2 provide hierarchical geographic information, corresponding to specific localities (e.g., province or site) and broader regions (e.g., country or ocean). The Section field records the name of the outcrop or drill core from which samples were collected. For records younger than 720 Ma, Paleolatitude and Paleolongitude were reconstructed using the GPlates Web Service (https://gws.gplates.org/) and the PALEOMAP plate reconstruction model (Scotese, 2021). These fields enable spatial analyses within both modern and paleogeographic frameworks and facilitate investigation of long-term geographic patterns in sedimentary Hg records.

https://doi.org/10.5194/essd-2026-511
Preprint. Discussion started: 21 September 2026

3.3 Chronostratigraphic information

Chronostratigraphic fields integrate numerical ages together with hierarchical stratigraphic classifications, including Era, Period, Epoch, Stage, Formation, and other stratigraphic descriptors (e.g., Unit) when available. Numerical ages were standardized according to the International Chronostratigraphic Chart (GTS v202412) (Cohen et al., 2025), ensuring consistency among records derived from different studies. The Unit field identifies specific stratigraphic intervals or geological events when reported. Era, Period, Epoch, and Stage describe the hierarchical stratigraphic framework, with Epoch and Stage used for Phanerozoic samples and broader divisions applied to Precambrian intervals where finer resolution is not available. The Formation field records the geological unit from which samples were collected, providing stratigraphic context. Together, these fields provide a unified temporal framework for investigating Hg variability across geological timescales while preserving the original stratigraphic context.

3.4 Lithological and depositional information

Lithological and depositional fields describe the sedimentological context of each sample. Lithology records the sediment type reported in the original publication, including shale, mudstone, and limestone, chert, and other sedimentary lithologies. Depositional-setting distinguish among marine, terrestrial systems, lacustrine, and other environmental settings where information is available. Relative depth describing stratigraphic position within individual sections preserves relative sample locations and enable high-resolution analyses of vertical variability. Together, these fields provide essential geological context for interpreting Hg concentrations and isotope compositions.

3.5 Geochemical information

Geochemical fields constitute the core scientific content of DeepSedHg and include Hg concentrations, Hg isotope compositions, and associated geochemical proxies. Hg concentrations are reported in ppb, whereas Hg isotope compositions, including δ^{xxx}Hg (xxx=199, 200, 201, 202, and 204) and Δ^{xxx}Hg (xxx=199, 200, 201, and 204), are reported in per mil (‰). The uncertainty fields record the reported 2σ uncertainties associated with individual Hg isotope parameters. To support interpretation of Hg host phases, the database also contains commonly reported normalization proxies, including TOC, TS, Al concentrations in wt %, and derived indices such as Hg/TOC, Hg/TS, and Hg/Al ratios in ppb/%. Additional geochemical variables include major (e.g., P, K, and Na in wt %) and trace element (in ppm) concentrations, stable isotope such as δ^{18}O (‰) and δ^{13}C (‰), and iron-speciation parameters reported in the source studies. Iron speciation fields include concentrations and ratios of operationally defined iron pools, such as pyrite iron (Fe_{py}), highly reactive iron (Fe_{HR}), total iron (Fe_T), and ratios such as Fe_{py}/Fe_{HR} and Fe_{HR}/Fe_T, which provide redox and depositional context (Poulton, 2021). Collectively, the geochemical variables enable integrated analyses of Hg abundance, isotope systematics, host-phase controls, and associated environmental conditions.

https://doi.org/10.5194/essd-2026-511
Preprint. Discussion started: 21 September 2026

Open Access Earth System Science Data Discussions

4 Data coverage and characteristics

4.1 Data source overview

DeepSedHg v1.0 integrates data from 199 peer-reviewed publications between 2010 and February 2026 (Figure 2). The number of source studies and compiled data entries increased markedly during the past decade, reflecting the rapid expansion of sedimentary Hg research and the growing application of Hg isotopes in Earth-system investigations. The compiled database contains 28,264 sample-level records, including 27,990 Hg concentration measurements and 3,969 Hg isotope measurements. The annual number of publications reached its highest values during 2021–2023, whereas data-entry production remained high during 2021–2025, showing that recent studies commonly reported larger datasets with higher sampling resolution.

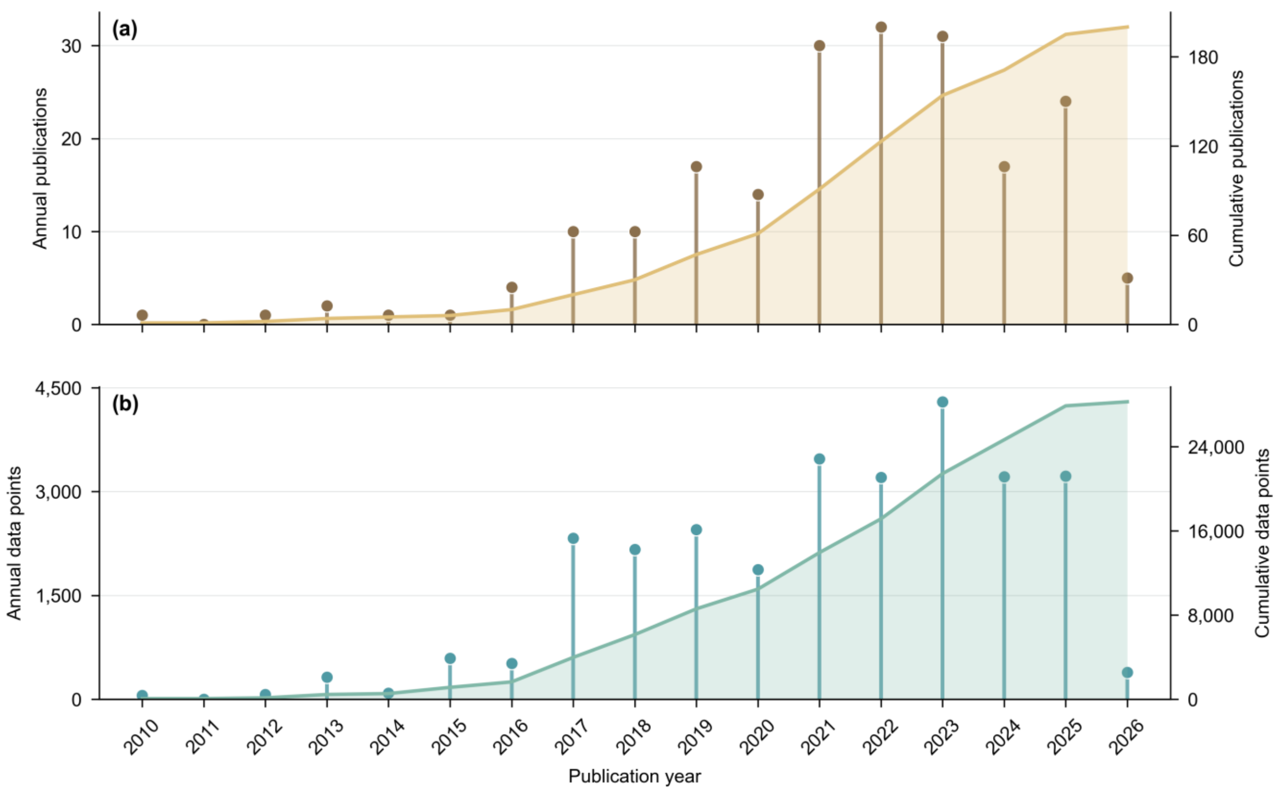

Figure 2. Data-source and time coverage of DeepSedHg database.

(a) Annual and cumulative numbers of source publications included in the database. (b) Annual and cumulative numbers of sample-level data entries. Vertical stems and circles represent annual counts, whereas shaded areas and solid curves represent cumulative totals.

https://doi.org/10.5194/essd-2026-511
Preprint. Discussion started: 21 September 2026

4.2 Spatial and temporal coverage

The spatial coverage of DeepSedHg is broad but uneven in modern geographic space. A total of 357 individual sampling sites are represented in the modern map, including 215 sites with Hg concentration data only, 4 sites with Hg isotope data only, and 138 sites with both Hg concentration and isotope data (Figure 3). Modern geographic coordinates indicate substantial coverage in Europe and East Asia, whereas large areas of Africa, South America, Australia, and open oceans are comparatively underrepresented. Sampling sites are strongly concentrated in the Northern Hemisphere, which accounts for ~91% of individual sampling sites. The highest site densities occur in the 30–40° N, 20–30° N, and 40–50° N latitude bands, with 93, 80, and 78 sites, respectively. By contrast, the Southern Hemisphere is much more sparsely represented. This uneven distribution reflects both the availability of suitable sedimentary successions and the geographic focus of Hg geochemical investigations.

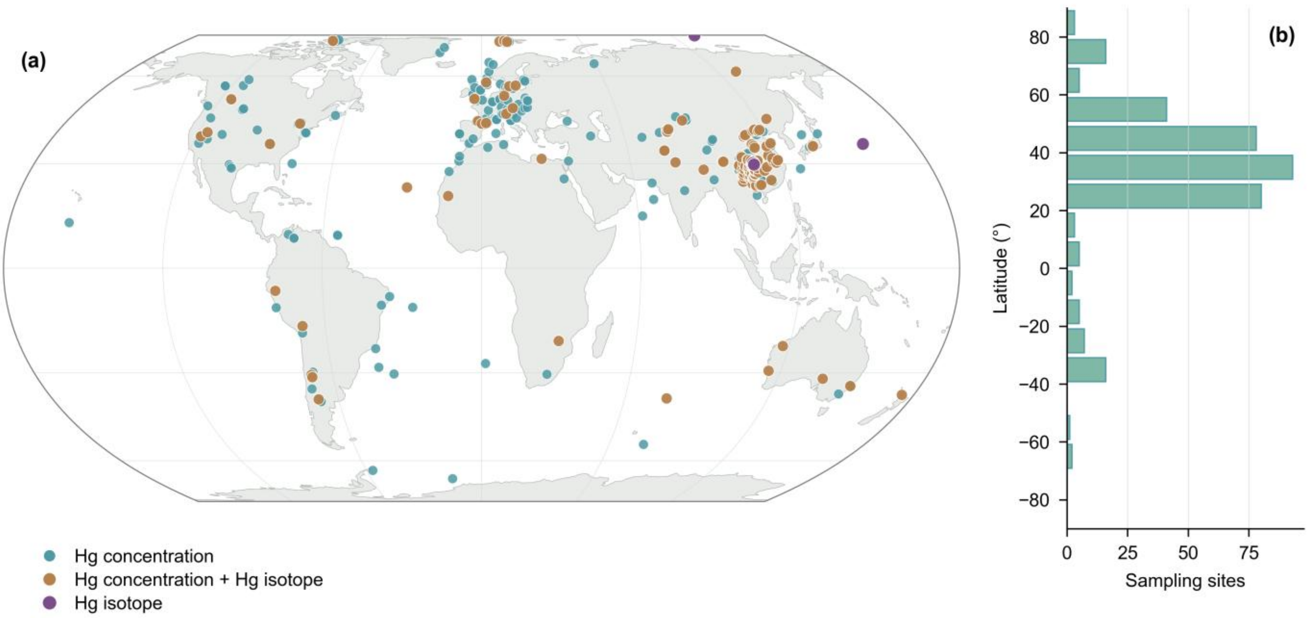

Figure 3. Modern spatial coverage of sampling sites in DeepSedHg database.
(a) Geographic distribution of sampling sites. (b) Latitudinal distribution of sampling sites binned in 10° latitude intervals.

The latitude–era heatmaps show that this unevenness varies through geological time (Figure 4). At the site level, Paleozoic records show the largest number of sites, with maxima of 50 sites at 20–30° N and 47 sites at 30–40° N (Figure 4a). Mesozoic records are also strongly concentrated in the Northern Hemisphere, especially at 40–50° N and 30–40° N, with 38 and 28 sites, respectively. Cenozoic sites are fewer but widely scattered, with the highest counts at 30–40° N. Precambrian sites are sparse overall, although they reach 18 sites at 20–30° N, indicating a limited but locally concentrated coverage. At the data-point level, heatmap shows a similar pattern (Figure 4b). The largest data-point clusters occur in the Paleozoic at

https://doi.org/10.5194/essd-2026-511
Preprint. Discussion started: 21 September 2026

30–40° N and 20–30° N, with 3,403 and 3,059 entries, respectively, and in the Mesozoic at 30–40° N and 40–50° N, with 2,677 and 3,051 entries. Cenozoic data are most abundant between 30° N and 60° N, but their counts are much lower than those of the Mesozoic and Paleozoic. Precambrian data points are limited to fewer latitude intervals, notably at 20–30° N and 40–50° N.

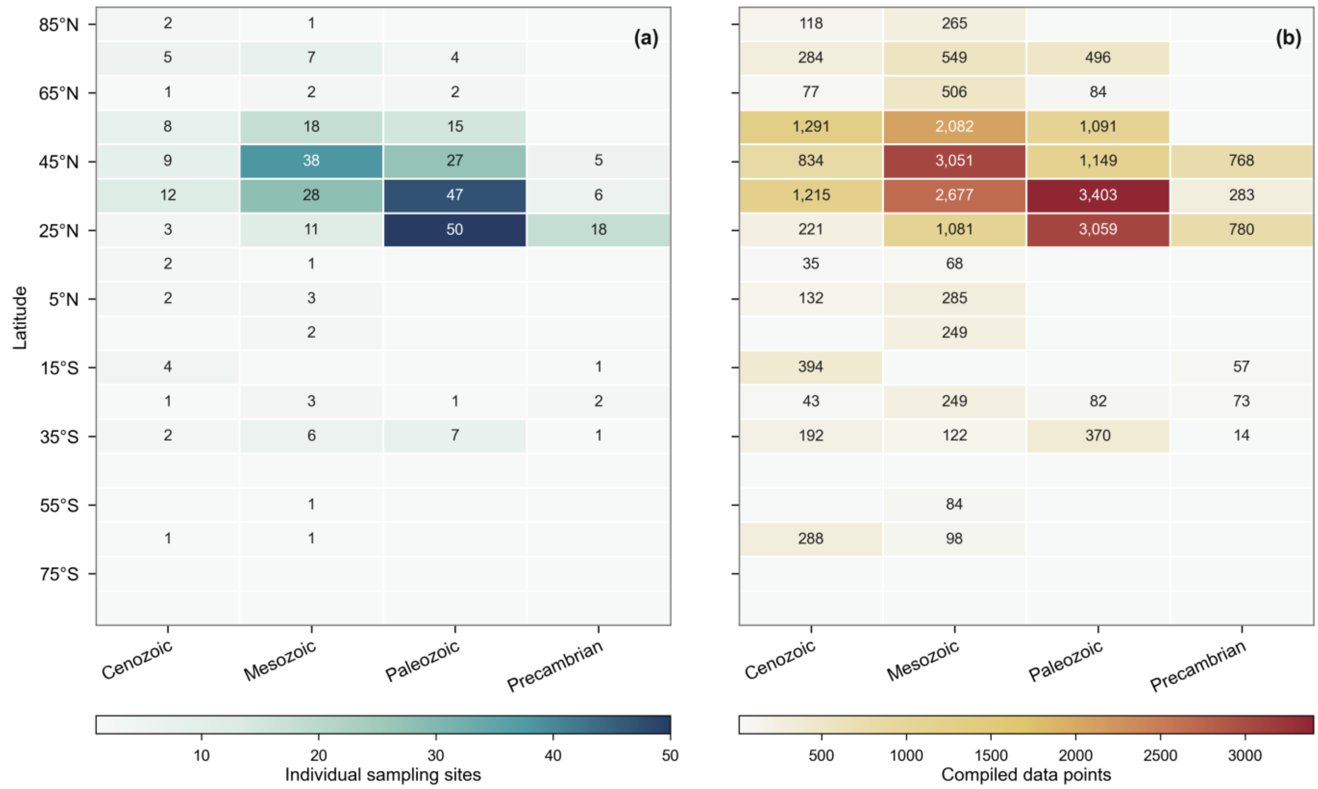

Figure 4. Latitudinal distribution of sampling sites and data points across major geological eras in DeepSedHg database. (a) Number of individual sampling sites binned in 10° latitude intervals at different geological eras. (b) Number of compiled data points binned in 10° latitude intervals at different geological eras.

To further assess spatial coverage, Phanerozoic records were plotted on period-level paleogeographic reconstructions (Figure 5). Compared with the modern geographic map, these reconstructions provide a more appropriate framework for evaluating sedimentary records in different plate configurations. The period-level maps show that Hg records occur across multiple reconstructed continental margins, ocean basins, and sedimentary provinces, but the spatial density and data-type vary substantially among periods.

https://doi.org/10.5194/essd-2026-511
Preprint. Discussion started: 21 September 2026

Open Access Earth System Science Data Discussions

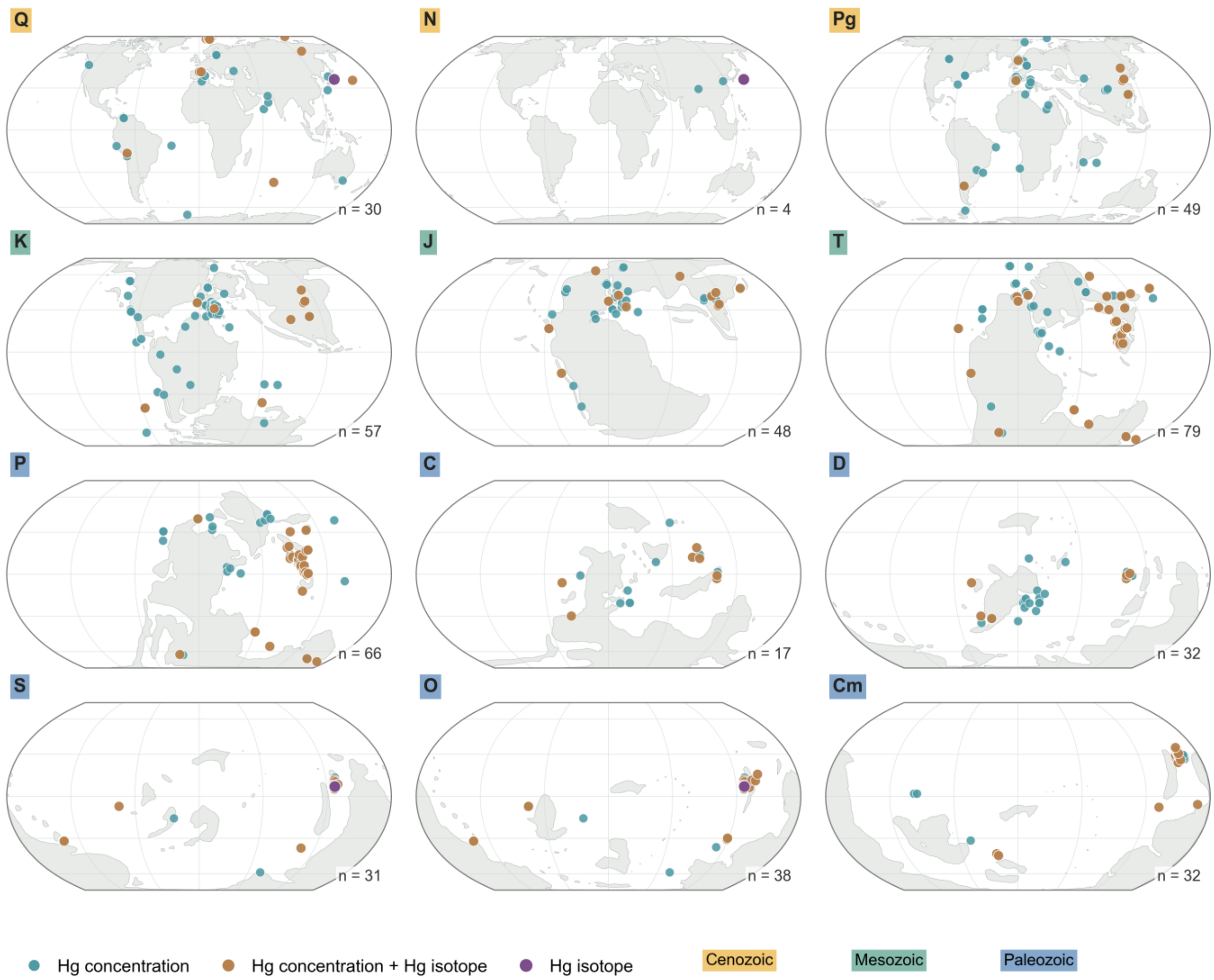

Figure 5. Phanerozoic paleogeographic distribution of Hg sampling sites in DeepSedHg database.

Each panel shows sampling sites reconstructed to their corresponding paleogeographic positions for one geological period. Period abbreviations: Q, Quaternary; N, Neogene; Pg, Paleogene; K, Cretaceous; J, Jurassic; T, Triassic; P, Permian; C, Carboniferous; D, Devonian; S, Silurian; O, Ordovician; Cm, Cambrian.

In the Cenozoic, Quaternary, Neogene, and Paleogene records are relatively scattered. The Paleogene contains the largest number of sites (n = 49) due to intensive studies on Paleocene-Eocene thermal maximum (PETM) events, whereas the Neogene is represented by only 3 sites. The Mesozoic panels show denser and more regionally clustered coverage. The Triassic contains the largest number of sites (n = 79), including 36 sites with both Hg concentration and isotope data, which is related to great interests into the mass extinction events in Permian-Triassic and Triassic-Cretaceous boundaries.

Cretaceous and Jurassic records are also well represented, with 57 and 48 sites, respectively, because there are numerous sedimentary successions relating to mass extinctions, oceanic anoxic events, and greenhouse intervals. Paleozoic records show a different pattern. The study sites focused mainly on the three mass extinction events, including Late Ordovician mass extinction (LOME), Late Devonian mass extinction (LDME), End Permian mass extinction (ETME). The Permian contains broad coverage, with 66 sites in total, including 35 sites with both Hg concentration and isotope data. Devonian and Cambrian records are moderate in number, with 32 sites each, but their distributions are more regionally clustered. Carboniferous records are comparatively sparse, with 17 sites. Silurian and Ordovician records contain even fewer total sites. Therefore, the temporal distribution across the Phanerozoic remains uneven, despite the extensive coverage. Periods with long histories of sedimentary geochemistry research are more densely represented than under-sampled periods, and users should consider potential temporal biases when conducting both event-scale and long-term analyses.

4.3 Characteristics of Hg concentration records

DeepSedHg contains 27,990 Hg concentration records and 3,920 records reporting at least one Hg isotope parameter. Of these, 23,340 Hg concentration records (~83%) and 3079 Hg isotope records (~79%) originate from marine sedimentary sections. Thus, these marine sedimentary records were presented below to provide a more comparable framework for evaluating the long-term trend of Hg concentrations and isotope compositions (Figures 6-8). Terrestrial sections are more likely affected by local sources and processes (Sun et al., 2023).

https://doi.org/10.5194/essd-2026-511
Preprint. Discussion started: 21 September 2026

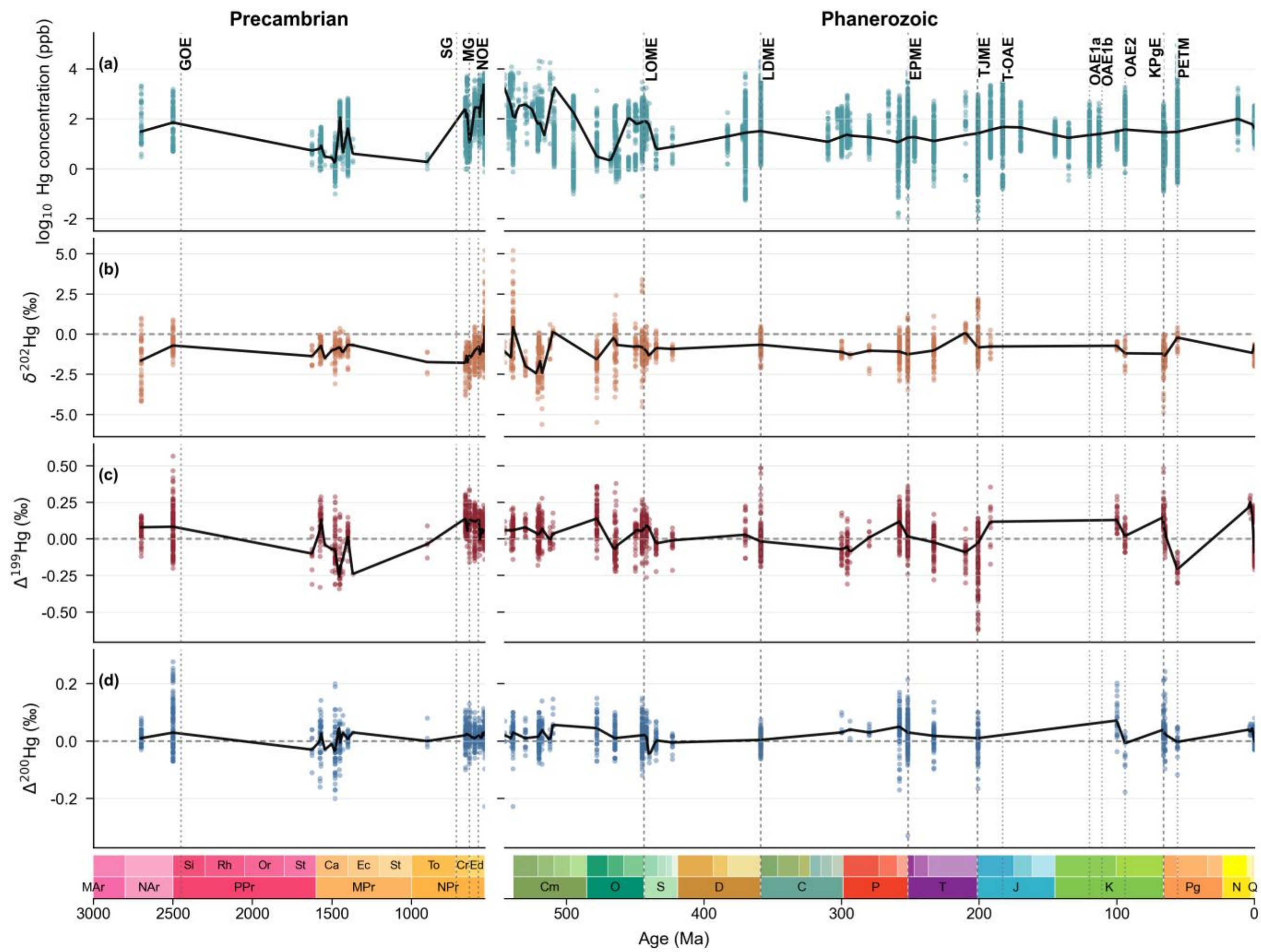

Figure 6. Temporal variations in Hg concentrations and Hg isotope composition values of marine sections in DeepSedHg database. (a) Hg concentration on a $\log_{10}$ scale, (b) δ^{202}Hg, (c) Δ^{199}Hg, and (d) Δ^{200}Hg plotted against geological age. Precambrian and Phanerozoic records are shown on separate x-axis scales. Points represent individual measurements, and black curves show LOWESS-smoothed trends based on age-specific median values. Dashed vertical lines mark key geological events, including Great Oxidation Event (GOE); Sturtian glaciation (SG); Marinoan glaciation (MG); Neoproterozoic Oxygenation Event (NOE); Late Ordovician mass extinction (LOME); Late Devonian mass extinction (LDME); End Permian mass extinction (EPME); Triassic-Jurassic mass extinction (TJME); Cretaceous-Paleogene mass extinction (KPgE); Toarcian Oceanic Anoxic Event (T-OAE); Oceanic Anoxic Event 1a (OAE1a); Oceanic Anoxic Event 1b (OAE1b); Oceanic Anoxic Event 2 (OAE2); and Paleocene-Eocene Thermal Maximum (PETM).

Mercury concentrations in the marine sedimentary records span several orders of magnitude, indicating strong heterogeneity among depositional settings and geological intervals (Figure 6a). Precambrian records generally exhibit higher Hg

https://doi.org/10.5194/essd-2026-511
Preprint. Discussion started: 21 September 2026

concentration than Phanerozoic records. The Precambrian dataset has a median Hg concentration of 40 ppb and an interquartile range (IQR: Q25-75) of 7–264 ppb, whereas the Phanerozoic dataset has a median of 32 ppb and an IQR of 11–82 ppb. The broader Precambrian distribution reflects scattered high values near the Archean–Paleoproterozoic transition and late Neoproterozoic intervals, rather than a uniformly elevated baseline. In the Phanerozoic, the Cambrian forms the most distinct high-Hg interval, with a median of 200 ppb, whereas Mesozoic records are generally lower, with median values of 23 ppb in the Triassic and 27 ppb in both the Jurassic and Cretaceous. Particularly, significant Hg enrichments occur near several critical geological events, including mass-extinction and oceanic anoxic events (Figure 6). Raw Hg concentration are strongly right-skewed, while Log_{10} transformation substantially reduces this skewness, producing broadly unimodal and more symmetric distributions (Figure 7a).

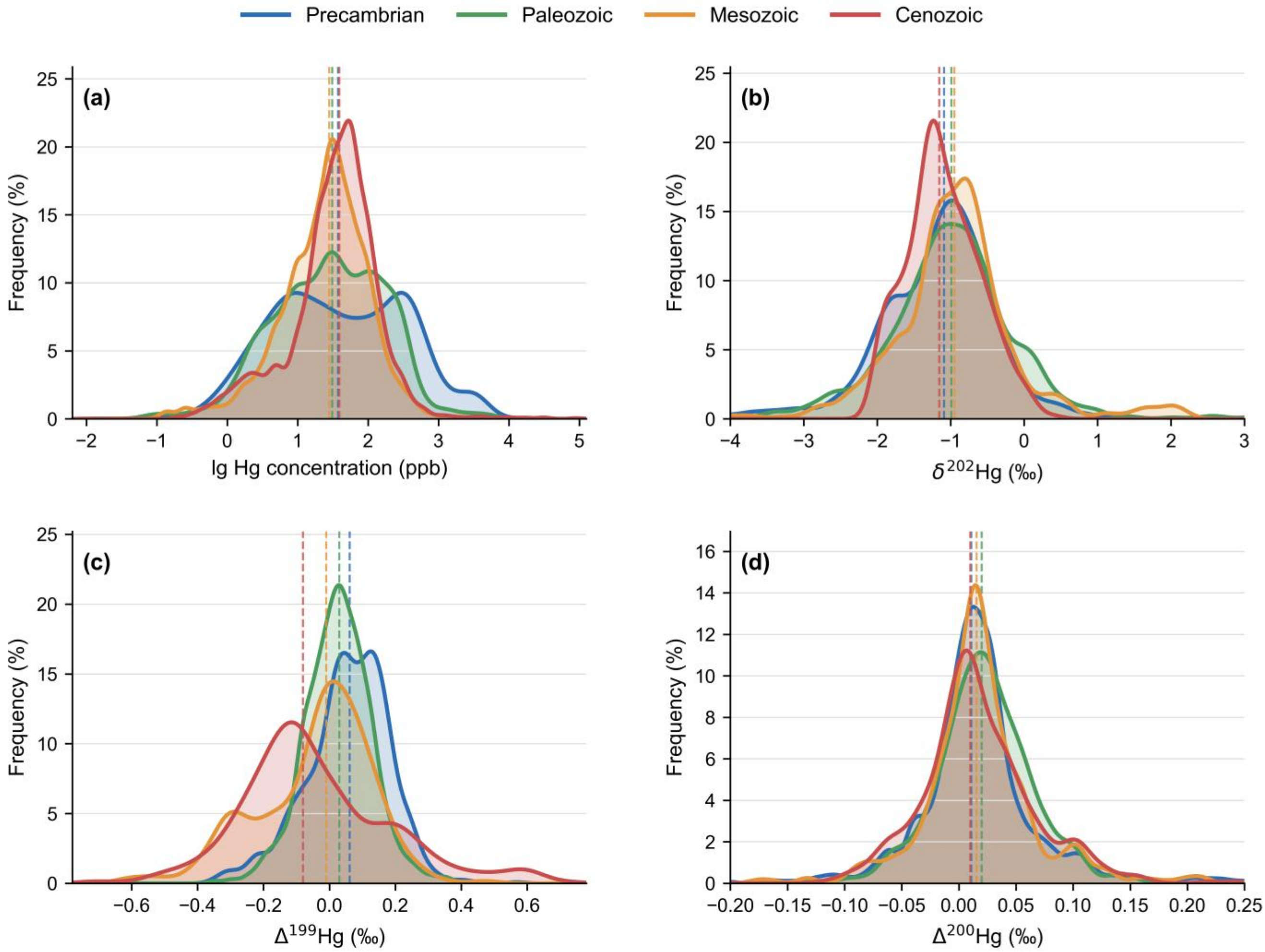

Figure 7. Frequency distributions of Hg concentrations and Hg isotope values in DeepSedHg database grouped by geological ages.

https://doi.org/10.5194/essd-2026-511
Preprint. Discussion started: 21 September 2026

(a) Hg concentration on a $\log_{10}$ scale, (b) δ^{202}Hg, (c) Δ^{199}Hg, and (d) Δ^{200}Hg. Colored curves represent smoothed frequency distributions for Precambrian, Paleozoic, Mesozoic, and Cenozoic records; dashed lines indicate median values for each group.

4.4 Characteristics of Hg isotope records

Compared with Hg concentration data, isotope records are more limited in temporal and spatial coverage, but they provide additional constraints on Hg sources and environmental processes. δ^{202}Hg, representing MDF, in marine sedimentary records ranges from -5.61‰ to 5.20‰ and is generally negative, with a median of -1.02‰ and an IQR of -1.50‰ to -0.58‰ (Figures 6b, 7b). Precambrian and Phanerozoic records have similar median values of -1.07‰ and -1.01‰, respectively, indicating that δ^{202}Hg does not show a simple long-term directional shift. Instead, it varies largely at an interval scale. Around the major geological events such as the “five big” mass extinctions, δ^{202}Hg values exhibit substantial fluctuations in response massive environmental changes (Figure 6b). Among well-sampled intervals, the most negative median δ^{202}Hg values occur in the Cambrian (-1.73‰) and Cryogenian (-1.72‰). Quaternary and Permian records also exhibit relatively negative median values of -1.22‰ and -1.18‰, respectively (Figure 6b). Δ^{199}Hg, representing odd-MIF, shows a clearer temporal and distributional contrast (Figures 6c, 7c). All marine sedimentary records have a median Δ^{199}Hg of 0.04‰ and an IQR of -0.04‰ to 0.11‰. Precambrian records have a median of 0.08‰ (IQR = 0.00‰ to 0.15‰), whereas Phanerozoic records have a lower median of 0.03‰ (IQR = -0.05‰ to 0.09‰). The most positive values occur near the Archean–Paleoproterozoic transition, reaching up to 0.57‰, while the most negative values occur near the end-Triassic interval, reaching down to -0.62‰. The Mesozoic–Cenozoic interval is one of the clearest examples of Δ^{199}Hg shifts. Cretaceous records are shifted toward positive Δ^{199}Hg values, with a median of 0.13‰. In contrast, Paleogene records have a near-zero median of -0.04‰, and Quaternary records show a further shift to -0.08‰ (Figure 6c). Δ^{200}Hg, representing even-MIF, remains much closer to zero than Δ^{199}Hg, with marine sedimentary records having a median of 0.018‰ and an IQR of -0.001‰ to 0.040‰ (Figures 6d, 7d). Precambrian and Phanerozoic records have similar median values of 0.016‰ and 0.019‰, respectively, indicating relatively weak temporal variation. Small positive Δ^{200}Hg deviations mainly clusters near the Archean-Paleoproterozoic transition and the end-Cretaceous interval (Figure 6d).

4.5 Relationships among Hg isotope parameters

The relationships among different Hg isotope values, including δ^{202}Hg vs. Δ^{199}Hg, Δ^{201}Hg vs. Δ^{199}Hg, and Δ^{200}Hg vs. Δ^{199}Hg, were illustrated using marine sedimentary records grouped by major geological ages (Figure 8). These relationships are commonly used to identify specific sources and environmental processes (Blum et al., 2014).

https://doi.org/10.5194/essd-2026-511
Preprint. Discussion started: 21 September 2026

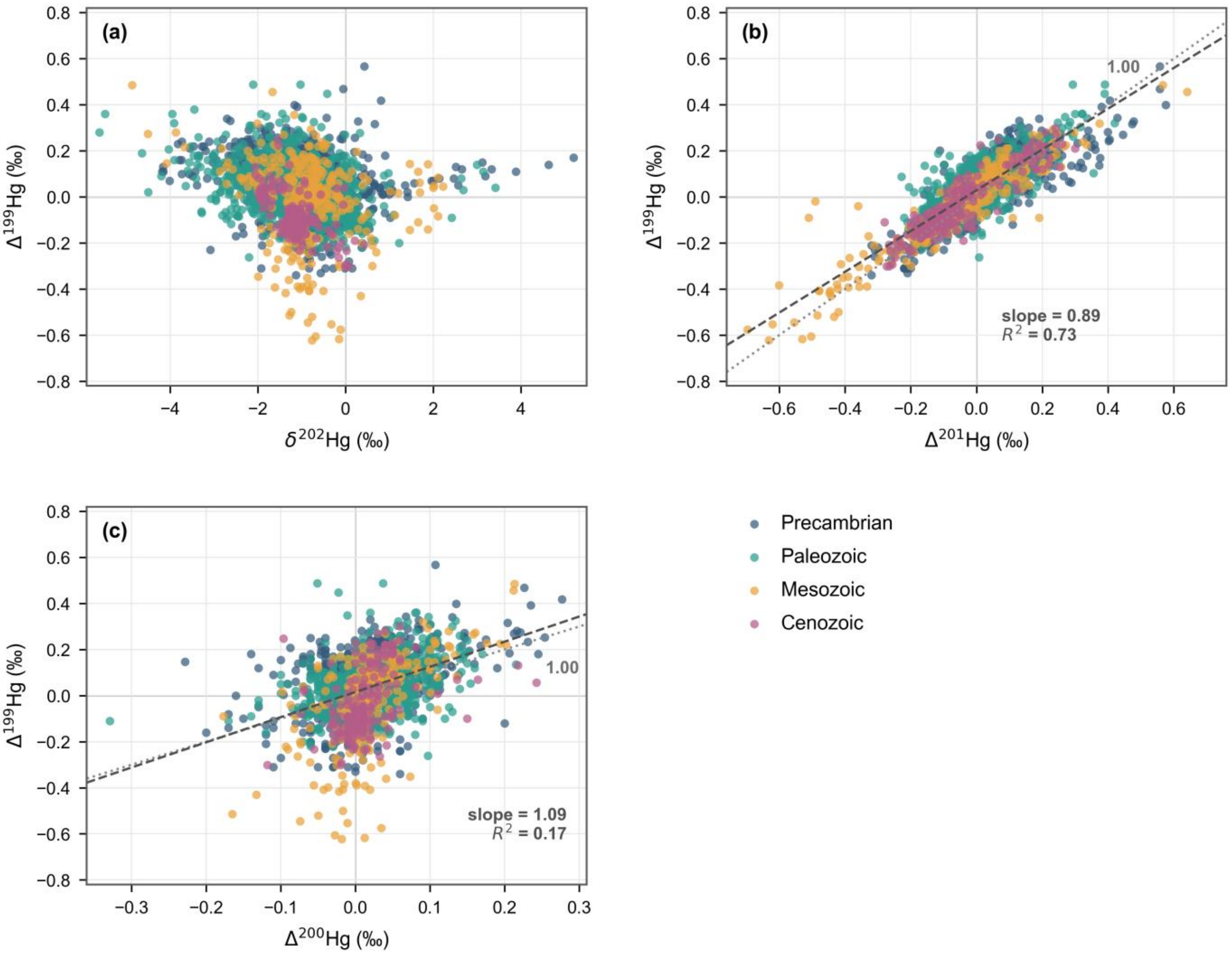

Figure 8. Relationships among Hg isotope values in marine sedimentary records of DeepSedHg database.
(a) δ^{202}Hg vs. Δ^{199}Hg, (b) Δ^{201}Hg vs. Δ^{199}Hg, (c) Δ^{200}Hg vs. Δ^{199}Hg. Colors denote major geological eras.

Records occupy a broad range of δ^{202}Hg values, which are dominantly negative, with comparatively narrower range of negative to positive Δ^{199}Hg and Δ^{200}Hg values. The δ^{202}Hg–Δ^{199}Hg distribution exhibits broad scatter and does not define a single dominant trend across the compiled dataset (Figure 8a). A clearer positive relationship is observed between Δ^{201}Hg and Δ^{199}Hg (Figure 8b). Most observations cluster near the 1:1 reference line, indicating broadly similar behavior between Δ^{201}Hg and Δ^{199}Hg. The relationship between Δ^{200}Hg and Δ^{199}Hg is weaker but remains generally positive (Figure 8c). These cross-isotope relationships provide a descriptive overview of the isotope data structure contained within DeepSedHg and may assist users in selecting subsets of records for future investigations.

5 Data usability, limitations, and potential applications

DeepSedHg provides a comprehensive and standardized compilation of sedimentary Hg concentration and isotopic data spanning approximately 2.7 billion years of Earth history. By integrating measurements from 199 peer-reviewed publications within a unified database framework, the dataset improves discoverability, accessibility, interoperability, and reusability of published Hg records and supports a wide range of applications in Earth-system science.

5.1 Data usability

A major strength of DeepSedHg lies in the integration of geochemical measurements with extensive geological and spatial metadata. In addition to Hg concentrations and isotope compositions, the database includes chronostratigraphic information, lithological descriptions, depositional settings, geographic coordinates, paleogeographic reconstructions, and associated geochemical proxies. This standardized structure enables users to identify, filter, and compare records across diverse geological intervals and environmental settings. Because all records are organized using consistent field definitions and machine-readable formats, DeepSedHg can be readily integrated into statistical, geospatial, and computational workflows. The database is suitable for applications ranging from exploratory data analysis and visualization to quantitative synthesis, temporal trend analysis, spatial mapping, and large-scale meta-analyses.

The inclusion of both Hg concentration and isotope data further enhances the utility of the compilation. Users may investigate Hg abundance patterns alone or combine concentration and isotope measurements to examine broader geochemical relationships across multiple temporal and spatial scales. The database therefore provides a flexible framework for addressing questions related to Hg cycling, volcanism, paleoenvironmental change, stratigraphic correlation, and Earth-system evolution. In addition, the preservation of sample-level observations and original bibliographic information ensures complete traceability to source publications. Users can therefore verify individual records, access original analytical details, and construct customized subsets tailored to specific research objectives.

5.2 Potential applications

DeepSedHg is intended to support a broad range of scientific applications. At the global scale, the database enables investigation of long-term patterns in sedimentary Hg concentrations and isotope compositions across geological time. The extensive temporal coverage facilitates comparative analyses among major geological intervals, including mass extinctions, oceanic anoxic events, greenhouse climates, and background environmental states. At regional and local scales, the database can be used to evaluate spatial variability in Hg distributions among depositional basins, paleogeographic settings, and lithological environments. The availability of geographic and paleogeographic coordinates also supports integration with plate-tectonic reconstructions and Earth-system modeling frameworks. The database is additionally well suited for data-driven research approaches. Standardized metadata and harmonized field structures facilitate implementation of statistical learning, network analysis, clustering methods, and other computational techniques that require consistent data formats.

https://doi.org/10.5194/essd-2026-511
Preprint. Discussion started: 21 September 2026

Future integration with complementary geochemical, stratigraphic, paleontological, and paleoenvironmental databases may further expand opportunities for interdisciplinary research.

5.3 Limitations

Despite its broad coverage and standardized structure, several limitations should be considered when using the dataset. First, spatial coverage is uneven. Sampling locations are concentrated in regions that have been extensively investigated during the past decade, including North America, Europe, and East Asia. Other regions remain comparatively underrepresented. Consequently, geographic distributions within the database should not be interpreted as direct representations of global Hg variability. Second, temporal coverage is heterogeneous. Certain geological intervals are represented by numerous studies and high sample densities, whereas others contain relatively sparse observations. Differences in record numbers may influence apparent temporal trends and should be considered when conducting quantitative analyses. Third, analytical methodologies vary among source publications. Although all studies were screened and standardized during compilation, DeepSedHg does not systematically harmonize laboratory-specific analytical information such as digestion procedure, extraction methods, instrument configurations, calibration protocols, detection limit or quality-control metrics. Variations among analytical workflows may affect the comparability of individual measurements, particularly for low-concentration samples and samples with complex matrix and subtle isotope variations (Shi et al., 2023; Sun et al., 2025). Fourth, metadata completeness varies among studies. While extensive efforts were made to recover missing information from original publications and supplementary materials, some records lack complete geological, geographic, or analytical context. Users conducting highly specialized analyses should consult the original publications for additional details when necessary. Finally, paleogeographic reconstructions are inherently uncertain and become progressively less constrained with increasing geological age. Paleocoordinates included in DeepSedHg should therefore be regarded as approximate reconstructions suitable for large-scale analyses rather than precise location estimates.

5.4 Future development

DeepSedHg is designed as a living and extensible database that can be updated as new data become available. Future releases will incorporate newly published Hg concentration and isotope records, improve geographic and temporal coverage, and expand metadata completeness where additional information can be recovered. Several enhancements are planned for future versions. These include more comprehensive analytical metadata, expanded documentation of quality-control information, additional geochemical proxy variables, and improved interoperability with other community databases and Earth-system data infrastructures. As sedimentary Hg research continues to expand, periodic updates will ensure that DeepSedHg remains a current and reliable resource for the Earth-science community. The long-term objective is to establish an openly accessible and community-maintained reference database that supports reproducible, transparent and data-driven investigations of Hg cycling and environmental change throughout Earth history.

Overall, DeepSedHg provides a traceable, quality-controlled, and FAIR-aligned framework for integrating sedimentary Hg records across geological time. While users should consider the limitations associated with data availability, analytical heterogeneity, and sampling biases, the database represents a substantial step toward improving access to and reuse of published Hg concentration and isotope data at the global scale.

Code availability

The Python scripts and plotting data used to generate Figures 1–8 are publicly available from the project GitHub repository at https://github.com/TJUYyc/DeepSedHg.

Data availability

The DeepSedHg database (version 1.0) is publicly available through Zenodo at https://doi.org/10.5281/zenodo.20713398 (Yang et al., 2026). The archived dataset contains the complete database in comma-separated value (CSV) format and a ReadMe file describing variable definitions, units, data structure, usage notes, and citation information. An online tool for browsing, filtering, visualizing, and extracting the data is available at https://deepsedhg.pages.dev.

Author contribution

R.S. conceived and supervised the project. Y.Y. conducted the literature survey, compiled the database, performed data harmonization and quality-control procedures, and prepared the initial manuscript draft. R.S. contributed to database design, data interpretation, and manuscript development. S. L. contributed to data visualization. W.Z., Y.L., and J.C. contributed to database evaluation, manuscript revision, and scientific discussion. All authors reviewed, edited, and approved the final manuscript.

Competing interests

The authors declare that they have no conflict of interest.

Financial support

This study is supported by the National Key Research and Development Program of China (2022YFF0800300; 2023YFF0807104) and National Natural Science Foundation of China (42421003, 42373011).

https://doi.org/10.5194/essd-2026-511
Preprint. Discussion started: 21 September 2026

References

Blum, J. D. and Bergquist, B. A.: Reporting of variations in the natural isotopic composition of mercury, Anal Bioanal Chem, 388, 353–359, https://doi.org/10.1007/s00216-007-1236-9, 2007.

Blum, J. D., Sherman, L. S., and Johnson, M. W.: Mercury Isotopes in Earth and Environmental Sciences, Annu. Rev. Earth Planet. Sci., 42, 249–269, https://doi.org/10.1146/annurev-earth-050212-124107, 2014.

Cohen, K., Harper, D., Gibbard, P., and Car, N.: The ICS international chronostratigraphic chart this decade, Episodes, 48, 105–115, https://doi.org/10.18814/epiiugs/2025/025001, 2025.

Driscoll, C. T., Mason, R. P., Chan, H. M., Jacob, D. J., and Pirrone, N.: Mercury as a Global Pollutant: Sources, Pathways, and Effects, Environ. Sci. Technol., 47, 4967–4983, https://doi.org/10.1021/es305071v, 2013.

Du, Y., Song, H., Algeo, T. J., Zhang, H., Peng, J., Wu, Y., Lai, J., Shu, X., Song, H., Wei, L., Zhang, J., Stüeken, E. E., Grasby, S. E., Dal Corso, J., Liu, X., Chu, D., Tian, L., Liang, Q., Li, X., Yao, H., and Song, H.: The global Deep-time Sediment Nitrogen Isotopes in Marine Systems (DSMS-NI) database, Earth Syst. Sci. Data, 18, 675–690, https://doi.org/10.5194/essd-18-675-2026, 2026.

Fendley, I. M., Frieling, J., Mather, T. A., Ruhl, M., Hesselbo, S. P., and Jenkyns, H. C.: Early Jurassic large igneous province carbon emissions constrained by sedimentary mercury, Nat. Geosci., 17, 241–248, https://doi.org/10.1038/s41561-024-01378-5, 2024.

Frieling, J.: Effects of redox variability and early diagenesis on marine sedimentary Hg records, Geochimica et Cosmochimica Acta, 2023.

Gong, Q., Ling, M.-X., and Zheng, W.: Applications of mercury stable isotopes for tracing volcanism in the geologic record, Sci. China Earth Sci., 67, 1436–1458, https://doi.org/10.1007/s11430-023-1236-8, 2024.

Grasby, S. E., Them, T. R., Chen, Z., Yin, R., and Ardakani, O. H.: Mercury as a proxy for volcanic emissions in the geologic record, Earth-Science Reviews, 196, 102880, https://doi.org/10.1016/j.earscirev.2019.102880, 2019.

Kwon, S. Y., Blum, J. D., Yin, R., Tsui, M. T.-K., Yang, Y. H., and Choi, J. W.: Mercury stable isotopes for monitoring the effectiveness of the Minamata Convention on Mercury, Earth-Science Reviews, 203, 103111, https://doi.org/10.1016/j.earscirev.2020.103111, 2020.

Li, S., Grasby, S. E., Xing, Y., Jarzembowski, E. A., Wang, Q., Zhang, H., Wan, X., and Wang, B.: Mercury contents and isotope ratios in marine and terrestrial archives across the Cretaceous/Paleocene boundary, Earth-Science Reviews, 248, 104635, https://doi.org/10.1016/j.earscirev.2023.104635, 2024.

Obrist, D., Kirk, J. L., Zhang, L., Sunderland, E. M., Jiskra, M., and Selin, N. E.: A review of global environmental mercury processes in response to human and natural perturbations: Changes of emissions, climate, and land use, Ambio, 47, 116–140, https://doi.org/10.1007/s13280-017-1004-9, 2018.

Percival, L. M. E., Tedeschi, L. R., Creaser, R. A., Bottini, C., Erba, E., Giraud, F., Svensen, H., Savian, J., Trindade, R., Coccioni, R., Frontalini, F., Jovane, L., Mather, T. A., and Jenkyns, H. C.: Determining the style and provenance of magmatic activity during the Early Aptian Oceanic Anoxic Event (OAE 1a), Global and Planetary Change, 200, 103461, https://doi.org/10.1016/j.gloplacha.2021.103461, 2021.

Poulton, S. W.: The Iron Speciation Paleoredox Proxy, Elements in Geochemical Tracers in Earth System Science, https://doi.org/10.1017/9781108847148, 2021.

Pyle, D. M. and Mather, T. A.: The importance of volcanic emissions for the global atmospheric mercury cycle, Atmospheric Environment, 37, 5115–5124, https://doi.org/10.1016/j.atmosenv.2003.07.011, 2003.

Scotese, C. R.: An Atlas of Phanerozoic Paleogeographic Maps: The Seas Come In and the Seas Go Out, Annu. Rev. Earth Planet. Sci., 49, 679–728, https://doi.org/10.1146/annurev-earth-081320-064052, 2021.

Selin, N. E.: Global Biogeochemical Cycling of Mercury: A Review, Annual Review of Environment and Resources, 34, 43–63, https://doi.org/10.1146/annurev.environ.051308.084314, 2009.

Shen, J., Chen, J., Algeo, T. J., Feng, Q., Yu, J., Xu, Y.-G., Xu, G., Lei, Y., Planavsky, N. J., and Xie, S.: Mercury fluxes record regional volcanism in the South China craton prior to the end-Permian mass extinction, Geology, 49, 452–456, https://doi.org/10.1130/G48501.1, 2021.

Shen, J., Chen, J., Yu, J., Algeo, T. J., Smith, R. M. H., Botha, J., Frank, T. D., Fielding, C. R., Ward, P. D., and Mather, T. A.: Mercury evidence from southern Pangea terrestrial sections for end-Permian global volcanic effects, Nat Commun, 14, 6, https://doi.org/10.1038/s41467-022-35272-8, 2023.

Shi, M., Bergquist, B. A., Zhou, A., Zhao, Y., Sun, R., Chen, J., and Zheng, W.: The efficiency of Hg cold vapor generation and its influence on Hg isotope analysis by MC-ICP-MS, J. Anal. At. Spectrom., 38, 1076–1087, https://doi.org/10.1039/D3JA00056G, 2023.

Sial, A. N., Gaucher, C., Filho, M. A. D. S., Ferreira, V. P., Pimentel, M. M., Lacerda, L. D., Filho, E. V. S., and Cezario, W.: C-, Sr-isotope and Hg chemostratigraphy of Neoproterozoic cap carbonates of the Sergipano Belt, Northeastern Brazil, Precambrian Research, 182, 351–372, https://doi.org/10.1016/j.precamres.2010.05.008, 2010.

Sonke, J. E., Angot, H., Zhang, Y., Poulain, A., Björn, E., and Schartup, A.: Global change effects on biogeochemical mercury cycling, Ambio, 52, 853–876, https://doi.org/10.1007/s13280-023-01855-y, 2023.

Sonke, J. E., Kwon, S. Y., Demers, J. D., Zheng, W., Cho, M., Lee, H., Williams, D., Lepak, R. F., and Janssen, S. E.: The Global Observation System for Mercury dataset for mercury stable isotope signatures in environmental media, Sci Data, 13, 688, https://doi.org/10.1038/s41597-026-07035-3, 2026.

Sun, J., Zhao, Y., Bergquist, B. A., Li, P., Sun, R., Liu, Y., Chen, J., and Zheng, W.: High precision analysis of mercury isotopes at ultra-low concentrations using dry cold vapor generation-MC-ICP-MS, J. Anal. At. Spectrom., 40, 2251–2260, https://doi.org/10.1039/D5JA00220F, 2025.

Sun, R., Liu, Y., Sonke, J. E., Feifei, Z., Zhao, Y., Zhang, Y., Chen, J., Liu, C.-Q., Shen, S., Anbar, A. D., and Zheng, W.: Mercury isotope evidence for marine photic zone euxinia across the end-Permian mass extinction, Commun Earth Environ, 4, 159, https://doi.org/10.1038/s43247-023-00821-6, 2023.

https://doi.org/10.5194/essd-2026-511
Preprint. Discussion started: 21 September 2026

U.S. Environmental Protection Agency: Method 1631, Revision E: Mercury in Water by Oxidation, Purge and Trap, and Cold Vapor Atomic Fluorescence Spectrometry, Office of Water, United States Environmental Protection Agency, 2002.

U.S. Environmental Protection Agency: Method 7473: Mercury in Solids and Solutions by Thermal Decomposition, Amalgamation, and Atomic Absorption Spectrophotometry, United States Environmental Protection Agency, 2007.

Wilkinson, M. D., Dumontier, M., Aalbersberg, Ij. J., Appleton, G., Axton, M., Baak, A., Blomberg, N., Boiten, J.-W., Da Silva Santos, L. B., Bourne, P. E., Bouwman, J., Brookes, A. J., Clark, T., Crosas, M., Dillo, I., Dumon, O., Edmunds, S., Evelo, C. T., Finkers, R., Gonzalez-Beltran, A., Gray, A. J. G., Groth, P., Goble, C., Grethe, J. S., Heringa, J., 'T Hoen, P. A. C., Hooft, R., Kuhn, T., Kok, R., Kok, J., Lusher, S. J., Martone, M. E., Mons, A., Packer, A. L., Persson, B., Rocca-Serra, P., Roos, M., Van Schaik, R., Sansone, S.-A., Schultes, E., Sengstag, T., Slater, T., Strawn, G., Swertz, M. A., Thompson, M., Van Der Lei, J., Van Mulligen, E., Velterop, J., Waagmeester, A., Wittenburg, P., Wolstencroft, K., Zhao, J., and Mons, B.: The FAIR Guiding Principles for scientific data management and stewardship, Sci Data, 3, 160018, https://doi.org/10.1038/sdata.2016.18, 2016.

Yager, J. A., West, A. J., Thibodeau, A. M., Corsetti, F. A., Rigo, M., Berelson, W. M., Bottjer, D. J., Greene, S. E., Ibarra, Y., Jadoul, F., Ritterbush, K. A., Rollins, N., Rosas, S., Di Stefano, P., Sulca, D., Todaro, S., Wynn, P., Zimmermann, L., and Bergquist, B. A.: Mercury contents and isotope ratios from diverse depositional environments across the Triassic–Jurassic Boundary: Towards a more robust mercury proxy for large igneous province magmatism, Earth-Science Reviews, 223, 103775, https://doi.org/10.1016/j.earscirev.2021.103775, 2021.

Yang, Y., Li, S., Zheng, W., Liu, Y., Chen, J., and Sun, R.: DeepSedHg version 1.0: A global database of deep-time sedimentary mercury concentrations and isotope compositions, https://doi.org/10.5281/zenodo.20713398, 2026.

Yin, R., Feng, X., Li, X., Yu, B., and Du, B.: Trends and advances in mercury stable isotopes as a geochemical tracer, Trends in Environmental Analytical Chemistry, 2, 1–10, https://doi.org/10.1016/j.teac.2014.03.001, 2014.

Zheng, W., Gilleaudeau, G. J., Kah, L. C., and Anbar, A. D.: Mercury isotope signatures record photic zone euxinia in the Mesoproterozoic ocean, Proc. Natl. Acad. Sci. U.S.A., 115, 10594–10599, https://doi.org/10.1073/pnas.1721733115, 2018.

Zheng, W., Zhou, A., Sahoo, S. K., Nolan, M. R., Ostrander, C. M., Sun, R., Anbar, A. D., Xiao, S., and Chen, J.: Recurrent photic zone euxinia limited ocean oxygenation and animal evolution during the Ediacaran, Nat Commun, 14, 3920, https://doi.org/10.1038/s41467-023-39427-z, 2023.

Zhou, Y., Li, Y., Zheng, W., Tang, S., Pan, S., Chen, J., He, X.-F., Shen, J., and Algeo, T. J.: The role of LIPs in Phanerozoic mass extinctions: An Hg perspective, Earth-Science Reviews, 249, 104667, https://doi.org/10.1016/j.earscirev.2023.104667, 2024.